

Article

# Evaluation of Commercial “Carbon Quantum Dots” Sample on Origins of Red Absorption and Emission Features

Weixiong Liang <sup>1</sup>, Lin Ge <sup>1</sup>, Xiaofang Hou <sup>1</sup>, Xianyan Ren <sup>1</sup>, Liju Yang <sup>2,\*</sup>,  
Christopher E. Bunker <sup>3,\*</sup>, Christopher M. Overton <sup>1</sup>, Ping Wang <sup>1</sup> and Ya-Ping Sun <sup>1,\*</sup>

<sup>1</sup> Department of Chemistry and Laboratory for Emerging Materials and Technology, Clemson University, Clemson, SC 29634, USA; wliang@g.clemson.edu (W.L.); ge2@g.clemson.edu (L.G.); xiaofah@g.clemson.edu (X.H.); renxianyan@swust.edu.cn (X.R.); overtoncm@email.wofford.edu (C.M.O.); sungpr@clemson.edu (P.W.)

<sup>2</sup> Department of Pharmaceutical Sciences, Biomanufacturing Research Institute and Technology Enterprise, North Carolina Central University, Durham, NC 27707, USA

<sup>3</sup> Air Force Research Laboratory, Aerospace Systems Directorate, Wright-Patterson Air Force Base, Dayton, OH 45433, USA

\* Correspondence: liyang@nccu.edu (L.Y.); christopher.bunker@us.af.mil (C.E.B.); syaping@clemson.edu (Y.-P.S.)

Received: 19 September 2019; Accepted: 28 October 2019; Published: 1 November 2019



**Abstract:** The commercially acquired aqueous solution of “carbon quantum dots” sample was evaluated by optical absorption and fluorescence emission methods; in reference to aqueous dispersed small carbon nanoparticles and representative carbon dots prepared from chemical functionalization of the carbon nanoparticles. The results suggest a very low content of carbon that is associated with nanoscale carbon particles/domains in the as-supplied sample; and likely significant contamination by dye-like species/mixtures. In the absence of any information on the synthesis and history of the commercial sample, the possible cause of the contamination was illustrated by an example on similar dye formation in the one-pot carbonization synthesis of “red carbon dots” from citric acid–formamide precursor mixtures under too mild processing conditions that were insufficient for the intended carbonization. The negative impacts to the carbon dots research field by the apparent proliferation and now commercial availability of carbon-deficient or even largely carbon-less “carbon quantum dots”, which are more susceptible to dye contamination or dominance, are discussed.

**Keywords:** carbon dots; carbon quantum dots; commercial sample; dye contamination; carbonization

## 1. Introduction

Carbon dots (CDots) [1,2] which are generally defined as small carbon nanoparticles with various surface passivation schemes (Figure 1) [3] have attracted much attention, as reflected by the large and ever increasing number of relevant publications in the literature [4–15]. On the preparation of CDots, the originally reported dot samples were synthesized by chemically functionalizing pre-processed and selected small carbon nanoparticles [1,2], thus structurally adhering more closely or literally to the definition (Figure 1). However, the overwhelming majority of the reported syntheses since then have been based on various carbonization processes with organic and other carbon-containing species as precursors. These processes were generally not under conditions that would carbonize the precursors into soot-like materials composed of solid carbon nanoparticles, rather more like mixtures of some nanoscale carbon domains created as a result of the carbonization and the remaining organic species that survived the processing conditions. For such mixtures to be considered as dot samples,

an assumption relevant to the definition on CDots, whether implicitly or explicitly, is such that the net effect in these mixtures is essentially equivalent to the carbon domains passivated by the organic species in several possible modes. Among them could be organic attachments, adsorptions, and/or simple mixing in an “organic pool”. Again, collectively the interactions in all these modes might be considered as being in net effect similar to the carbon nanoparticle surface passivation schemes found in CDots from the chemical functionalization synthesis [16,17].

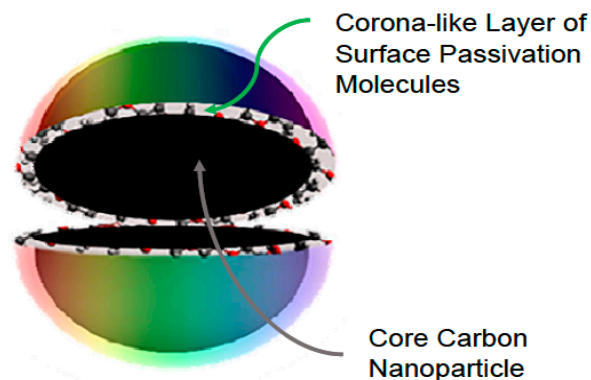


**Figure 1.** A cartoon illustration on the structure in carbon dots (CDots).

The equivalency assumption discussed above is necessary for the carbonization approach, because there are no theoretical (in terms of thermodynamic or kinetic driving forces) or experimental justifications for any expectation that the largely random and chaotic carbonization processing would produce the kind of well-ordered structures of solid carbon nanoparticles surface-functionalized by organic molecules or molecular segments. Consequently, the carbonization processing conditions must be critical to the compositions, especially the content of nanoscale carbon domains, and the interactions in the resulting product mixtures. In fact, recent investigations in the literature have raised questions on some reported dot samples obtained from “one-pot” carbonization syntheses [16,18–21] especially on those from thermal processing under very mild conditions such as “cooking a simple organic mixture at lower than 200 °C for a few hours”. Similarly mild one-pot carbonization conditions were used in some reported experiments on the synthesis of “red-absorptive and emissive” samples from some selected specific precursor mixtures [22–30] such as mixtures of citric acid with formamide [22,24] on which there are understandably concerns with respect to not only the content of nanoscale carbon domains and dot structures in such samples but also the potentially substantial interference from dye-like species produced in the processing. Meanwhile, the scientific chemical supplier MilliporeSigma has recently started to market the dot sample of red absorption and emission features from unspecified source(s) or production method. Commercial availability of CDots can be very positive to the further development and applications in this research field and beyond, but at the same time bring significant risks to users who are not equipped to judge and verify the sample structure and composition that are claimed to be responsible for the observed absorption and emission properties.

In the work reported here, we evaluated the “carbon quantum dots” sample solution supplied by MilliporeSigma and found only a small amount of carbon in the sample that could be associated with nanoscale carbon particles or domains, which obviously must be the key ingredient in any carbon-based/derived quantum dots. The experimental results led to the conclusion that the as-supplied sample must be dominated by dye-like species/mixtures, regardless of their detailed structural arrangements with the small amount of carbon in the sample. In the absence of any information on the sample history, the likely cause of the dominating contamination was illustrated by an example on similar dye formation in some of the recently reported one-pot carbonization syntheses of “red carbon dots” from specifically selected precursor mixtures under too mild processing conditions that were insufficient for the desired carbonization. The hope is for the supplier to provide customers with solid evidence proving that the marketed sample is indeed “carbon quantum dots” in terms of the dot

structure and chemical composition. As related, the dangers for the proliferation of carbon-deficient or even largely carbon-less “carbon quantum dots” (thus more vulnerable to dye contamination or dominance) to cause serious damages to the relevant research fields are highlighted and discussed.

## 2. Experimental Section

### 2.1. Materials

The “carbon quantum dots” sample as a 10 mL aqueous solution (product #900414, lot #MKCK3040) was purchased from MilliporeSigma (Burlington, MA, USA). Carbon nanopowders (US1074) were acquired from USA Research Nanomaterials, Inc. (Houston, TX, USA). Nitric acid, citric acid, formamide, and DMF were obtained from VWR International (Radnor, PA, USA), thionyl chloride (>98%) from TCI America (Portland, OR), and 2,2'-(ethylenedioxy)bis(ethylamine) (EDA) from MilliporeSigma (Burlington, MA, USA). Dialysis membrane tubing (molecular weight cut-off ~500) was supplied by Spectrum Laboratories (Rockleigh, NJ, USA). Water was deionized and purified in a Millipore Direct Q Water Purification System (Burlington, MA, USA).

### 2.2. Measurement

UV/vis/near-IR absorption spectra were recorded on Shimadzu UV-2501 and UV-3600 spectrophotometers (Columbia, MD, USA). Fluorescence spectra were acquired on a Jobin-Yvon emission spectrometer (Piscataway, NJ, USA) equipped with a 450 W xenon source, Gemini-180 excitation and Triax-550 emission monochromators, and a photon counting detector (Hamamatsu R928P PMT at 950 V). 9,10-Bis(phenylethynyl)anthracene in cyclohexane was used as a standard in the determination of fluorescence quantum yields by the relative method (matching the absorbance at the excitation wavelength between the sample and standard solutions and comparing their corresponding integrated total fluorescence intensities).

### 2.3. Thermal Processing of Citric Acid (CA)–Formamide (FA)

CA (0.5 g) was mixed with (dissolved in) FA (8.4 mL) under mild sonication (briefly in a VWR 250D ultrasonic cleaner). The resulting colorless solution was stirred in a round-bottom flask with three necks (one fitted with a glass condenser, one for temperature monitoring, and the other for purging with nitrogen). The stirring was at 160 °C under nitrogen protection for 1 h. The resulting dark-red colored solution was allowed to be back at room temperature for characterization and measurements.

For the thermal processing at 300 °C, the same CA–FA mixture was loaded into a small stainless steel tube reactor from Swagelok (Atlanta, GA, USA). The reactor was sealed and then heated in a tube furnace at 300 °C for 2 h. Post-processing, the reaction mixture in the reactor back at ambient temperature was collected by washing with water (10 mL). The resulting aqueous suspension was briefly centrifuged at 1000× *g*, and the supernatant was used for characterization and measurements.

### 2.4. EDA-CDots

The same synthetic protocol and post-synthesis processing and characterizations as those reported previously [31] were used for the EDA-CDots sample. Briefly on the synthesis, a sample of the pre-processed and selected small carbon nanoparticles (50 mg) was refluxed in neat thionyl chloride for 12 h. Upon the removal of excess thionyl chloride via evaporation, the resulting sample was carefully mixed with EDA (1 g), heated to 120 °C, and stirred vigorously under nitrogen protection for 72 h. The reaction mixture was cooled to room temperature and dispersed in water, and then centrifuged at 20,000× *g* for 1 h to retain the supernatant. The aqueous solution thus obtained was dialyzed against fresh water (molecular weight cut-off ~500) to remove unreacted EDA and other small molecular species to yield the EDA-CDots as an aqueous solution.

### 3. Results and Discussion

The as-supplied dot sample from MilliporeSigma was an aqueous solution of a very light pink color (Figure 2). The optical absorption spectrum of the as-supplied solution was measured in a standard 1.0 cm cuvette, and the observed absorbances were  $\sim 0.12$  at 400 nm and  $\sim 0.054$  at 480 nm (Figure 2). The absorption spectrum featured a very broad band around 480 nm, which would probably qualify the sample to be in the rank of “red-absorptive” (or more accurately “longer wavelength-absorptive” for the absorption band not quite in the red yet) [22–30]. Since it is well known that electronic transitions responsible for the observed optical absorptions in solid carbon nanoparticles are dominated by  $\pi$ -plasmons [32–35] the known absorption spectrum of aqueous dispersed carbon nanoparticles is shown for comparison [31]. Additionally shown in Figure 2 is the absorption spectrum of the CDots sample from chemical functionalization of the carbon nanoparticles with 2,2'-(ethylenedioxy)bis(ethylamine) (EDA) [31,36]. The EDA-CDots have been thoroughly characterized and often served as a benchmark in the research and development of CDots, and their optical absorptions are understandably similar to those of the carbon nanoparticles, as compared in Figure 2, because there are no theoretical and technical reasons to expect any significant alterations to  $\pi$ -plasmons in the carbon nanoparticles due to the surface functionalization by organic molecules. Thus, the implied assignment of the broad absorption band around 480 nm in the spectrum of MilliporeSigma sample (Figure 2) to the nano-carbon in “carbon quantum dots” is questionable, as it would require major changes to the  $\pi$ -plasmons intrinsic to nanoscale carbon allotropes including not only carbon nanoparticles but also carbon nanotubes [34,37]. In fact, the sample contained only a very small amount of nano-carbon according to the observed absorbances of the sample solution.

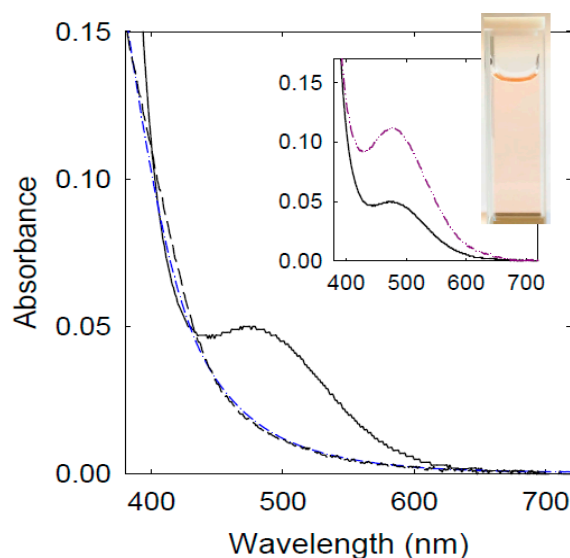


**Figure 2.** The absorption spectrum of the as-supplied MilliporeSigma sample solution (measured five days after the sample was received, solid line) compared with those of the aqueous dispersed small carbon nanoparticles (dash line, from reference 17) and EDA-CDots (dash-dot-dash line). Inset: The same absorption spectrum of the as-supplied MilliporeSigma sample solution (solid line) compared with the spectrum of the same sample solution measured six weeks after (dash-dot-dot-dash line). Moreover, in the inset is a photo of the as-supplied sample solution.

The insensitivity of  $\pi$ -plasmons in carbon nanoparticles towards effects of surface functionalization and the like is reflected by the general consistency in observed absorptivity values of the nanoparticles from different sources and also post-functionalization in CDots. The experimentally determined molar absorptivity values of aqueous dispersed carbon nanoparticles and their corresponding CDots are 50–100 (or roughly  $75 \pm 25$ )  $M_C^{-1} \text{cm}^{-1}$  over 400–420 nm, where  $M_C$  is the carbon molar concentration, namely the absorptivity measured in terms of the molar concentration of carbon atoms in the carbon

nanoparticles [38,39]. For the MilliporeSigma sample solution, the observed absorption at 400 nm (Figure 2) was more likely a combination of absorption due to the nano-carbon (carbon in the nanoscale carbon particles/domains) and the tail of the broad band around 480 nm. However, even under the assumption that the absorption was due entirely to the nano-carbon, the calculated “nanoparticle carbon” content (excluding carbon atoms in organic species) in the as-supplied sample solution was only  $\sim 0.02$  mg/mL (0.002% by weight or 20 ppm), namely at the maximum only about 0.2 mg of nanoscale carbon particles/domains in the as-supplied 10 mL sample solution. Thus, the as-supplied sample was likely produced under mild processing conditions without sufficient carbonization.

The very low nano-carbon content in the MilliporeSigma sample added more questions on the species responsible for the broad absorption band around 480 nm (Figure 2), which could not be associated with CDots for sure. A simple explanation would be the contamination by some dye-like species/mixtures that were produced in the synthesis of the dot sample, and the explanation is supported by results from fluorescence emission measurements.

As well known in the literature, fluorescence spectra and quantum yields of CDots are excitation wavelength dependent in a rather characteristic pattern (Figures 3 and 4) [1,17,35]. For the MilliporeSigma sample, the pattern for the spectral change with excitation wavelength was largely similar to that of EDA-CDots, except for excitations around 460 nm (Figure 3). At 460 nm excitation, there were some relatively minor additional emission contributions on top of the “normal” fluorescence band, due likely to some of the “longer wavelength-absorptive” species in the sample. As expected, the underlying fluorescence emissions for 460 nm excitation responded differently to the presence of a quencher. For example, the observed fluorescence spectrum in the presence of 0.15 M 2,4-dinitrotoluene (DNT) [17] was obviously different from that in the absence of the quencher (Figure 3 inset). In fact, the spectrum with the DNT quenching seemed more “normal” in its fit into the excitation wavelength dependence pattern (Figure 3).

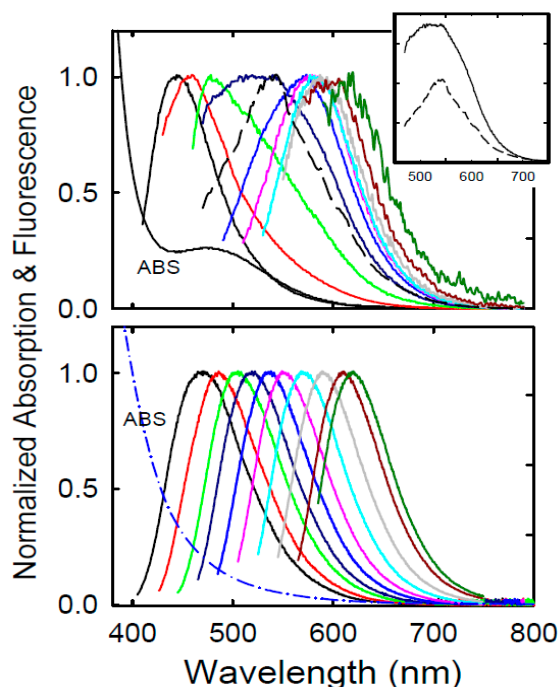


**Figure 3.** Upper: Absorption (ABS) and normalized fluorescence spectra at different excitation wavelengths (from 400 to 580 nm in the 20 nm increment) of the as-supplied MilliporeSigma sample solution. The fluorescence spectrum at 460 nm excitation in the presence of 0.15 M 2,4-dinitrotoluene as quencher is shown in the same normalized scale (dash line), and also in the insert in the relative intensity scale for comparison. Lower: Absorption (ABS) and fluorescence spectra at different excitation wavelengths (from 400 to 580 nm in the 20 nm increment) of EDA-CDots in aqueous solution.

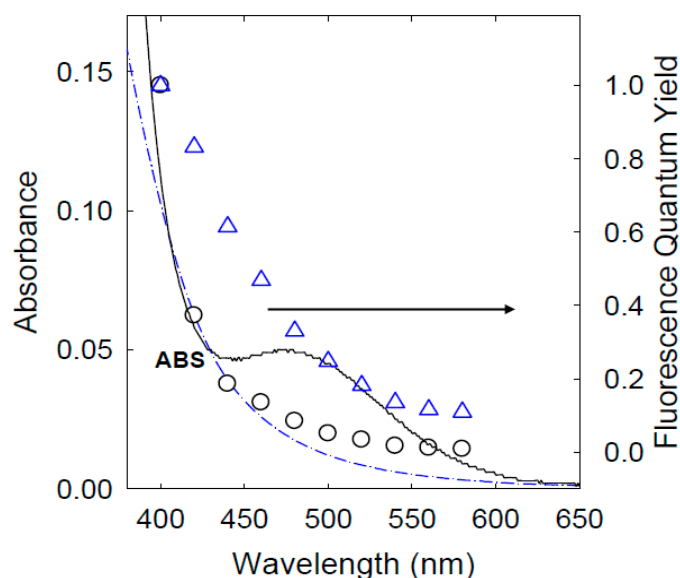


**Figure 4.** Fluorescence quantum yields at different excitation wavelengths of the as-supplied MilliporeSigma sample solution (○) are compared with those of EDA-CDots (△), where the yields are normalized against the values at 400 nm excitation of 5.9% for the former and 24% for the latter. Their absorption spectra (solid line for the former, and dash-dot-dash line for the latter) are also shown.

The fluorescence quantum yields of the MilliporeSigma sample were progressively lower at longer excitation wavelengths (5.9% at 400 nm excitation and 0.2% at 520 nm excitation), in a pattern similar to that for EDA-CDots, but the decrease was more rapid (Figure 4). Unlike in the spectral changes with excitation wavelengths discussed above, there was no obvious exception for excitations around 460 nm in the progressive decreases of fluorescence quantum yields. These results suggest that the MilliporeSigma sample was “longer wavelength-absorptive”, but hardly “longer wavelength-emissive”. As discussed above, the observed absorption spectrum of the sample solution was likely a superposition of the typical nano-carbon absorptions (Figure 2) and the broad visible absorption band associated with dye-like species/mixtures. The latter according to the fluorescence results were only weakly emissive or non-emissive, thus making the observed fluorescence quantum yields appear lower than what they should be (Figure 4, because the absorptions of the weakly emissive or non-emissive species were included in the calculation of observed quantum yields, similar to the classical “inner-filter effect” in fluorescence quantum yield determination based on the relative method).

It should also be pointed out that the observed absorption spectrum of the MilliporeSigma sample changed over time, such as the obvious difference from the time of sample arrival to about six weeks later (Figure 2 inset). There were some corresponding changes in the fluorescence spectra and quantum yields, but not substantial to the level that would fundamentally alter the excitation wavelength dependence patterns.

Collectively the results presented above are consistent with the notion that the sample solution acquired from MilliporeSigma contained dye-like species/mixtures responsible for the significant visible absorption band on top of the relatively weak absorptions by some nano-carbon in probably a CDots-like configuration (Figure 2), but these dye-like species/mixtures were only weakly fluorescent in general. The observed absorption spectral changes over time (Figure 2 inset) also suggest that regardless of the identities and compositions of these species/mixtures, they were unstable under the ambient storage conditions. Despite the absence of any information on the synthesis method and protocol for the MilliporeSigma sample, a safe assumption is that the sample was produced under processing conditions insufficient for the required carbonization, thus vulnerable to contamination by dye-like species/mixtures formed in the processing. This may be illustrated by the similar dye

formation and contamination in the synthesis of “red-carbon dots” from citric acid–formamide mixtures with carbonization processing conditions insufficient for the desired CDots.

Among syntheses reported in the literature for dot samples of absorption and fluorescence emission bands extended into the red or even near-IR spectral region, citric acid (CA) has been a popular component in mixtures with some specifically selected organic molecules such as formamide (FA) to be used as precursor for carbonization [22,24,29,40]. Equally popular in the carbonization of these precursor mixtures has been the use of rather mild thermal processing conditions of less than 200 °C for up to a few hours, such as in a microwave-heated bath at 160 °C for an hour for CA–FA mixtures specifically [22,24]. These processing conditions were obviously incapable of producing the claimed “red carbon dots”, as demonstrated in the work reported here by a simple comparison between the same thermal processing at 160 versus 300 °C.

For the processing at 160 °C, a CA–FA mixture (essentially a solution of CA in FA) was stirred in a setup designed for refluxing for an hour, during which the solution color changed from largely colorless to dark red. The optical absorption spectrum of the solution upon dilution is shown in Figure 5. The spectrum is not the same as those reported in the literature for samples obtained from comparable processing conditions (though the spectra of those samples in the literature were actually very different among themselves) [22,24] but nevertheless with the similar absorption feature of extra visible bands not found in the absorption spectrum of carbon nanoparticles or EDA-CDots (Figure 5). The observed fluorescence spectra and quantum yields are still excitation wavelength dependent (Figures 5 and 6), but not in the commonly found characteristic patterns [17,35], likely reflecting contributions by species associated with the extra visible absorption bands.

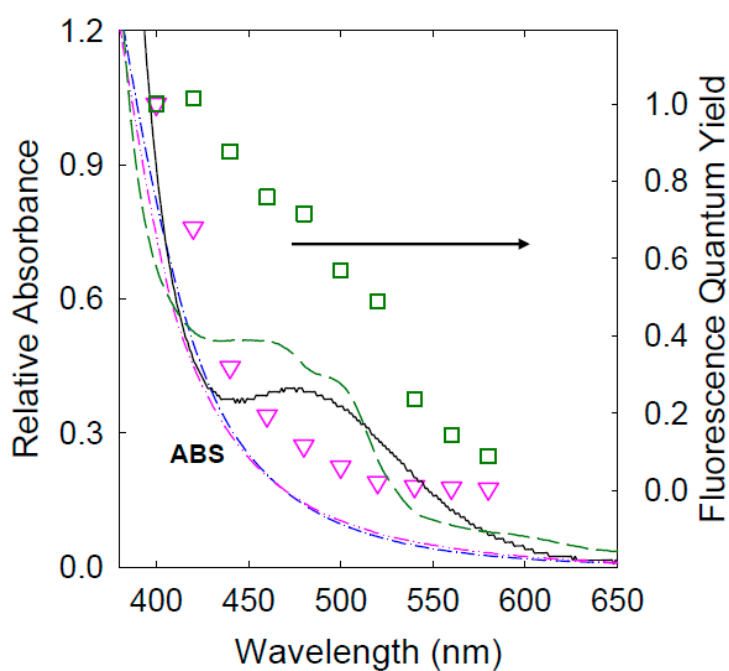


**Figure 5.** Absorptions (ABS) and fluorescence quantum yields at different excitation wavelengths of the two samples from processing the citric acid–formamide (CA–FA) mixture at 160 °C for 1 h (dash line and  $\square$ ) and at 300 °C for 2 h (dash-dot-dot-dash line and  $\nabla$ ) are compared, where the yields are normalized against the values at 400 nm excitation of 20% for the former and 14% for the latter. The normalized absorption spectra of the as-supplied MilliporeSigma sample solution (solid line and  $\bullet$ ) and EDA-CDots (dash-dot-dash line) are also shown for comparison.

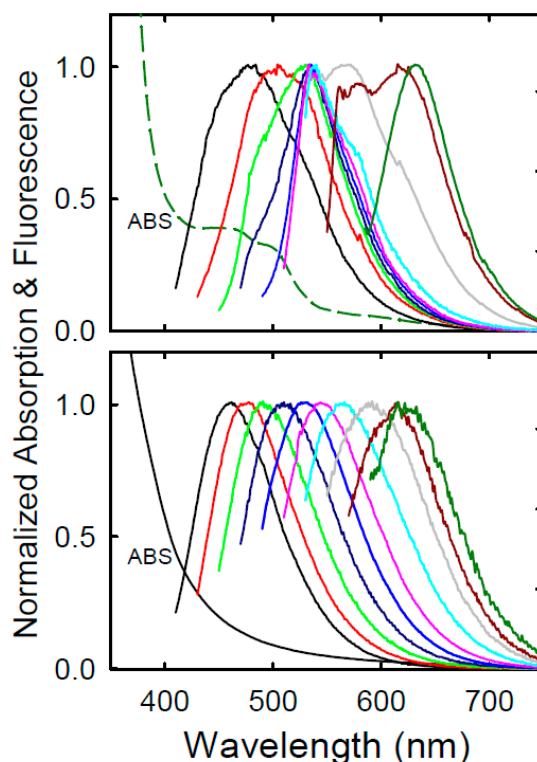


**Figure 6.** Absorption (ABS) and fluorescence spectra at different excitation wavelengths (from 400 to 580 nm in the 20 nm increment) of the two samples from processing the CA–FA mixture at 160 °C for 1 h (upper) and at 300 °C for 2 h (lower) are compared.

One might wonder if the extra visible absorption bands (Figure 5, Supplementary Materials) and the corresponding fluorescence properties (Figure 6) could actually be due to the sample being populated by “red-carbon dots”, as claimed in the literature [22,24]. Unfortunately, the answer would have to be a resounding no, because these features could only be found in the samples produced under the mild processing conditions. Even in terms of just common sense, these processing conditions would not be sufficient for any substantial carbonization, let alone altering the electronic transitions dominated by  $\pi$ -plasmons of nano-carbon in the desired dot structure. In fact, these extra absorption and fluorescence emission features were simply fading away with increasing temperature and time in the carbonization processing, consistent with the expected decomposition and/or carbonization of the initially formed dye-like species/mixtures. For example, by processing the same CA–FA mixture at 300 °C for 2 h, the absorption spectrum of the resulting sample became rather similar to those of the dispersed carbon nanoparticles and the established CDots like EDA-CDots, namely no extra longer wavelength visible absorption bands anymore (Figure 5). Correspondingly, the excitation wavelength dependence of fluorescence spectra reverted back to the characteristic pattern (Figure 6), and so did the dependence of fluorescence quantum yields (Figure 5) [35]. These findings suggest that in the one-pot thermal processing, significantly more robust conditions than those used in many of the reported studies are necessary in order to ensure sufficient carbonization of the organic precursors. As a result, these properly prepared dot samples will exhibit the same absorption characteristics as those of the pre-existing small carbon nanoparticles, with the corresponding fluorescence emission properties similar to those of CDots derived from the surface functionalization of the carbon nanoparticles.

The example highlighted above on the carbonization of CA–FA is hardly an exception, and the findings are relevant to the argument that the broad absorption band around 480 nm in the spectrum of the MilliporeSigma sample could not be genuine to any “longer-wavelength absorptive carbon dots”, rather due to dye-like species in potentially complex mixtures produced in the synthesis of the sample. The option of further processing the as-supplied sample under more robust carbonization conditions

(similar to those in the processing of the CA–FA mixture at a high temperature) was considered but deemed non-practical because the sample was already so dilute, barely enough for fluorescence measurements at near the detection limit of the emission spectrometer equipped with a sensitive photon-counting detector. The isolation and identification of the dye-like species in likely complex mixtures in the MilliporeSigma sample would be even more challenging. One might also argue that the supplier of the commercial sample would be best suited or even obligated for performing these tasks.

More broadly, the name and definition of *carbon* dots call for the dominance of *carbon* in the dot structure, where the *carbon* refers to the carbon nanoparticles or more generally nanoscale carbon domains in the dots, excluding the carbon atoms in organic species also presented in the dot structure for the passivation function (namely the surface passivation of the carbon nanoparticles or nanoscale carbon domains). Since the overwhelming majority of the dot syntheses have been based on the carbonization of organic precursors, utmost caution must be exercised in the syntheses to ensure a sufficient degree of carbonization for the necessary dominant presence of nanoscale carbon domains in the produced dot samples. Unfortunately, the required sufficient carbonization of organic matters is not as readily achieved as many may choose to believe, definitely not under some of the widely applied conditions like “cooking at one hundred and some degrees Celsius for an hour or so”. Such mild processing conditions cannot be sufficient to convert organic species into nanoscale carbon structures in any substantial fashion, let alone some claimed “crystalline or graphitic nanoparticles”. In fact, if this were possible, one would be producing a significant amount of carbon quantum dots in pan-frying or barbecuing some vegetables, or even better enjoying the taste of carbon quantum dots when sipping a cup of tea because the tea in that cup is often processed under conditions much more aggressive than those for the one-pot carbonization referred to above. One should also be mindful that carbon nanoparticles can readily be generated from organic matters *in situ* in an electron microscopy machine equipped with a powerful electron beam of up to 300 kV. Thus, “seeing” nanoparticles in electron microscopy images is hardly sufficient for “proving” the substantial presence of carbon quantum dots in samples from carbonization under rather mild processing conditions.

A serious consequence of the under-carbonization is the high probability of contamination or even dominance by dye-like species/mixtures formed as intermediate molecules and/or byproducts of the carbonization processing, though their presence becomes evident only when they are absorptive and/or fluorescent in the concerned spectral region, especially prominent in the red/near-IR because of the relatively low absorptivities of carbon nanoparticles at those wavelengths. To avoid these risks, the carbonization synthesis must focus on the creation of dominant nanoscale carbon domains, which are after all at the core (literally) of the desired carbon quantum dots.

The caution emphasized here is critical to the advancement of the research field on carbon-based/derived quantum dots, thus to avoid the pollution by results obtained with some poorly synthesized samples, including commercial products, which are mostly complex mixtures of dye-like species, including red-absorptive and/or emissive dyes, with perhaps only a sprinkle of small carbon pieces.

**Supplementary Materials:** The following are available online at <http://www.mdpi.com/2311-5629/5/4/70/s1>, Figure S1: Comparisons of absorption spectra and fluorescence quantum yields, Figure S2: Comprehensive comparisons of fluorescence spectra at different excitation wavelengths.

**Author Contributions:** Data acquisition & analyses, W.L., L.G., X.H., X.R., C.M.O., and P.W.; Funding acquisition, L.Y., and Y.-P.S.; Investigation, W.L., L.G., and P.W.; Project administration, Y.-P.S.; Supervision, L.Y., C.E.B., and Y.-P.S.; Validation, W.L.; Writing—original draft, W.L., L.G., and Y.-P.S.; Writing—review & editing, C.E.B., and Y.-P.S.

**Funding:** Air Force Office of Scientific Research, and National Science Foundation.

**Acknowledgments:** Financial support from Air Force Office of Scientific Research through the program of Kenneth Caster (FA9550-16-1-0166, Y.-P.S.) and NSF (1855905, L.Y.) is gratefully acknowledged. C.M.O. was a participant of Palmetto Academy (a summer undergraduate research program of the South Carolina Space Grant Consortium).

**Conflicts of Interest:** The authors declare no conflict of interest.

## References

1. Sun, Y.-P.; Zhou, B.; Lin, Y.; Wang, W.; Fernando, K.A.S.; Pathak, P.; Jaouad Meziani, M.; Harruff, B.A.; Wang, X.; Wang, H.; et al. Quantum-Sized Carbon Particles for Bright and Colorful Photoluminescence. *J. Am. Chem. Soc.* **2006**, *128*, 7756–7757. [[CrossRef](#)] [[PubMed](#)]
2. Sun, Y.-P. Fluorescent Carbon Nanoparticles. U.S. Patent 7,829,772 B2, 9 November 2010.
3. Cao, L.; Meziani, M.J.; Sahu, S.; Sun, Y.-P. Photoluminescence Properties of Graphene *versus* Other Carbon Nanomaterials. *Acc. Chem. Res.* **2013**, *46*, 171–180. [[CrossRef](#)] [[PubMed](#)]
4. Luo, P.G.; Sahu, S.; Yang, S.-T.; Sonkar, S.K.; Wang, J.; Wang, H.; LeCroy, G.E.; Cao, L.; Sun, Y.-P. Carbon “Quantum” Dots for Optical Bioimaging. *J. Mater. Chem. B* **2013**, *1*, 2116–2127. [[CrossRef](#)]
5. Ding, C.; Zhu, A.; Tian, Y. Functional Surface Engineering of C-Dots for Fluorescent Biosensing and in Vivo Bioimaging. *Acc. Chem. Res.* **2014**, *47*, 20–30. [[CrossRef](#)] [[PubMed](#)]
6. Luo, P.G.; Yang, F.; Yang, S.-T.; Sonkar, S.K.; Yang, L.; Broglie, J.J.; Liu, Y.; Sun, Y.-P. Carbon-Based Quantum Dots for Fluorescence Imaging of Cells and Tissues. *RSC Adv.* **2014**, *4*, 10791–10807. [[CrossRef](#)]
7. Lim, S.Y.; Shen, W.; Gao, Z. Carbon Quantum Dots and Their Applications. *Chem. Soc. Rev.* **2015**, *44*, 362–381. [[CrossRef](#)] [[PubMed](#)]
8. Fernando, K.A.S.; Sahu, S.; Liu, Y.; Lewis, W.K.; Gulians, E.A.; Jafariyan, A.; Wang, P.; Bunker, C.E.; Sun, Y.-P. Carbon Quantum Dots and Applications in Photocatalytic Energy Conversion. *ACS Appl. Mater. Interfaces* **2015**, *7*, 8363–8376. [[CrossRef](#)]
9. LeCroy, G.E.; Yang, S.-T.; Yang, F.; Liu, Y.; Fernando, K.A.S.; Bunker, C.E.; Hu, Y.; Luo, P.G.; Sun, Y.-P. Functionalized Carbon Nanoparticles: Syntheses and Applications in Optical Bioimaging and Energy Conversion. *Coord. Chem. Rev.* **2016**, *320*, 66–81. [[CrossRef](#)]
10. Peng, Z.; Han, X.; Li, S.; Al-Youbi, A.O.; Bashammakh, A.S.; El-Shahawi, M.S.; Leblanc, R.M. Carbon Dots: Biomacromolecule Interaction, Bioimaging and Nanomedicine. *Coord. Chem. Rev.* **2017**, *343*, 256–277. [[CrossRef](#)]
11. Hutton, G.A.M.; Martindale, B.C.M.; Reisner, E. Carbon Dots as Photosensitisers for Solar-Driven Catalysis. *Chem. Soc. Rev.* **2017**, *46*, 6111–6123. [[CrossRef](#)]
12. Namdari, P.; Negahdari, B.; Eatemadi, A. Synthesis, Properties and Biomedical Applications of Carbon-Based Quantum Dots: An Updated Review. *Biomed. Pharmacother.* **2017**, *87*, 209–222. [[CrossRef](#)] [[PubMed](#)]
13. Atabaev, T. Doped Carbon Dots for Sensing and Bioimaging Applications: A Minireview. *Nanomaterials* **2018**, *8*, 342. [[CrossRef](#)] [[PubMed](#)]
14. Molaei, M.J. A Review on Nanostructured Carbon Quantum Dots and Their Applications in Biotechnology, Sensors, and Chemiluminescence. *Talanta* **2019**, *196*, 456–478. [[CrossRef](#)] [[PubMed](#)]
15. Du, J.; Xu, N.; Fan, J.; Sun, W.; Peng, X. Carbon Dots for In Vivo Bioimaging and Theranostics. *Small* **2019**, *15*, 1805087. [[CrossRef](#)] [[PubMed](#)]
16. Hou, X.; Hu, Y.; Wang, P.; Yang, L.; Al Awak, M.M.; Tang, Y.; Twara, F.K.; Qian, H.; Sun, Y.-P. Modified Facile Synthesis for Quantitatively Fluorescent Carbon Dots. *Carbon* **2017**, *122*, 389–394. [[CrossRef](#)] [[PubMed](#)]
17. Ge, L.; Pan, N.; Jin, J.; Wang, P.; LeCroy, G.E.; Liang, W.; Yang, L.; Teisl, L.R.; Tang, Y.; Sun, Y.-P. Systematic Comparison of Carbon Dots from Different Preparations-Consistent Optical Properties and Photoinduced Redox Characteristics in Visible Spectrum and Structural and Mechanistic Implications. *J. Phys. Chem. C* **2018**, *122*, 21667–21676. [[CrossRef](#)]
18. Essner, J.B.; Kist, J.A.; Polo-Parada, L.; Baker, G.A. Artifacts and Errors Associated with the Ubiquitous Presence of Fluorescent Impurities in Carbon Nanodots. *Chem. Mater.* **2018**, *30*, 1878–1887. [[CrossRef](#)]
19. Xiong, Y.; Schneider, J.; Ushakova, E.V.; Rogach, A.L. Influence of Molecular Fluorophores on the Research Field of Chemically Synthesized Carbon Dots. *Nano Today* **2018**, *23*, 124–139. [[CrossRef](#)]
20. Khan, S.; Sharma, A.; Ghoshal, S.; Jain, S.; Hazra, M.K.; Nandi, C.K. Small Molecular Organic Nanocrystals Resemble Carbon Nanodots in Terms of Their Properties. *Chem. Sci.* **2018**, *9*, 175–180. [[CrossRef](#)]
21. Hinterberger, V.; Damm, C.; Haines, P.; Guldi, D.M.; Peukert, W. Purification and Structural Elucidation of Carbon Dots by Column Chromatography. *Nanoscale* **2019**, *11*, 8464–8474. [[CrossRef](#)]
22. Pan, L.; Sun, S.; Zhang, A.; Jiang, K.; Zhang, L.; Dong, C.; Huang, Q.; Wu, A.; Lin, H. Truly Fluorescent Excitation-Dependent Carbon Dots and Their Applications in Multicolor Cellular Imaging and Multidimensional Sensing. *Adv. Mater.* **2015**, *27*, 7782–7787. [[CrossRef](#)] [[PubMed](#)]

23. Jiang, B.-P.; Zhou, B.; Shen, X.-C.; Yu, Y.-X.; Ji, S.-C.; Wen, C.-C.; Liang, H. Selective Probing of Gaseous Ammonia Using Red-Emitting Carbon Dots Based on an Interfacial Response Mechanism. *Chem. Eur. J.* **2015**, *21*, 18993–18999. [[CrossRef](#)] [[PubMed](#)]
24. Sun, S.; Zhang, L.; Jiang, K.; Wu, A.; Lin, H. Toward High-Efficient Red Emissive Carbon Dots: Facile Preparation, Unique Properties, and Applications as Multifunctional Theranostic Agents. *Chem. Mater.* **2016**, *28*, 8659–8668. [[CrossRef](#)]
25. Chen, D.; Wu, W.; Yuan, Y.; Zhou, Y.; Wan, Z.; Huang, P. Intense Multi-State Visible Absorption and Full-Color Luminescence of Nitrogen-Doped Carbon Quantum Dots for Blue-Light-Excitable Solid-State-Lighting. *J. Mater. Chem. C* **2016**, *4*, 9027–9035. [[CrossRef](#)]
26. Qu, S.; Zhou, D.; Li, D.; Ji, W.; Jing, P.; Han, D.; Liu, L.; Zeng, H.; Shen, D. Toward Efficient Orange Emissive Carbon Nanodots through Conjugated  $sp^2$ -Domain Controlling and Surface Charges Engineering. *Adv. Mater.* **2016**, *28*, 3516–3521. [[CrossRef](#)] [[PubMed](#)]
27. Ge, J.; Jia, Q.; Liu, W.; Lan, M.; Zhou, B.; Guo, L.; Zhou, H.; Zhang, H.; Wang, Y.; Gu, Y.; et al. Carbon Dots with Intrinsic Theranostic Properties for Bioimaging, Red-Light-Triggered Photodynamic/Photothermal Simultaneous Therapy In Vitro and In Vivo. *Adv. Healthcare Mater.* **2016**, *5*, 665–675. [[CrossRef](#)] [[PubMed](#)]
28. Pan, L.; Sun, S.; Zhang, L.; Jiang, K.; Lin, H. Near-Infrared Emissive Carbon Dots for Two-Photon Fluorescence Bioimaging. *Nanoscale* **2016**, *8*, 17350–17356. [[CrossRef](#)]
29. Ding, H.; Wei, J.-S.; Zhong, N.; Gao, Q.-Y.; Xiong, H.-M. Highly Efficient Red-Emitting Carbon Dots with Gram-Scale Yield for Bioimaging. *Langmuir* **2017**, *33*, 12635–12642. [[CrossRef](#)]
30. Zhu, Z.; Zhai, Y.; Li, Z.; Zhu, P.; Mao, S.; Zhu, C.; Du, D.; Belfiore, L.A.; Tang, J.; Lin, Y. Red Carbon Dots: Optical Property Regulations and Applications. *Mater. Today* **2019**, in press. [[CrossRef](#)]
31. LeCroy, G.E.; Messina, F.; Sciortino, A.; Bunker, C.E.; Wang, P.; Fernando, K.A.S.; Sun, Y.-P. Characteristic Excitation Wavelength Dependence of Fluorescence Emissions in Carbon Quantum Dots. *J. Phys. Chem. C* **2017**, *121*, 28180–28186. [[CrossRef](#)]
32. Jäger, C.; Mutschke, H.; Henning, T.; Huisken, F. Spectral Properties of Gas-Phase Condensed Fullerene-Like Carbon Nanoparticles from Far-Ultraviolet to Infrared Wavelengths. *Astrophys. J.* **2008**, *689*, 249–259. [[CrossRef](#)]
33. Osipov, V.Y.; Baranov, A.V.; Ermakov, V.A.; Makarova, T.L.; Chungong, L.F.; Shames, A.I.; Takai, K.; Enoki, T.; Kaburagi, Y.; Endo, M.; et al. Raman Characterization and UV Optical Absorption Studies of Surface Plasmon Resonance in Multishell Nanographite. *Diam. Relat. Mater.* **2011**, *20*, 205–209. [[CrossRef](#)]
34. Osipov, V.Y.; Shestakov, M.S.; Baranov, A.V.; Ermakov, V.A.; Shames, A.I.; Takai, K.; Enoki, T.; Kaburagi, Y.; Hayashi, T.; Endo, M.; et al. Diagnostics of Plasmon Resonance in Optical Absorption Spectra of Nanographite Aqueous Suspensions. *Opt. Spectrosc.* **2011**, *111*, 220. [[CrossRef](#)]
35. Gupta, D.B.; Pathak, A.; Semwal, V. Carbon-Based Nanomaterials for Plasmonic Sensors: A Review. *Sensors* **2019**, *19*, 3536. [[CrossRef](#)]
36. LeCroy, G.E.; Sonkar, S.K.; Yang, F.; Veca, L.M.; Wang, P.; Tackett, K.N.; Yu, J.-J.; Vasile, E.; Qian, H.; Liu, Y.; et al. Toward Structurally Defined Carbon Dots as Ultracompact Fluorescent Probes. *ACS Nano* **2014**, *8*, 4522–4529. [[CrossRef](#)]
37. Cheung, W.; Patel, M.; Ma, Y.; Chen, Y.; Xie, Q.; Lockard, J.V.; Gao, Y.; He, H.  $\pi$ -Plasmon Absorption of Carbon Nanotubes for the Selective and Sensitive Detection of  $Fe^{3+}$  Ions. *Chem. Sci.* **2016**, *7*, 5192–5199. [[CrossRef](#)]
38. Xu, J.; Sahu, S.; Cao, L.; Anilkumar, P.; Tackett, K.N., II; Qian, H.; Bunker, C.E.; Gulians, E.A.; Parenzan, A.; Sun, Y.-P. Carbon Nanoparticles as Chromophores for Photon Harvesting and Photoconversion. *ChemPhysChem* **2011**, *12*, 3604–3608. [[CrossRef](#)]
39. Cao, L.; Shiral Fernando, K.A.; Liang, W.; Seilkop, A.; Monica Veca, L.; Sun, Y.-P.; Bunker, C.E. Carbon Dots for Energy Conversion Applications. *J. Appl. Phys.* **2019**, *125*, 220903. [[CrossRef](#)]
40. Lu, H.; Xu, S.; Liu, J. One Pot Generation of Blue and Red Carbon Dots in One Binary Solvent System for Dual Channel Detection of  $Cr^{3+}$  and  $Pb^{2+}$  Based on Ion Imprinted Fluorescence Polymers. *ACS Sens.* **2019**, *4*, 1917–1924. [[CrossRef](#)]

